A Numerical Discretization Method for the Dynamic Simulation of a Double-Pipe Heat Exchanger

Stefano Bracco, Ilka Faccioli, and Michele Troilo

Abstract—The present paper deals with both the steady-state and dynamic simulation of a double-pipe heat exchanger, in parallel-flow or counterflow arrangement. In particular, the article describes the thermodynamic model that has been implemented in the Matlab/Simulink environment; the main hypotheses and physical parameters, which characterize the simulation model, are listed. The paper is focused on the discretization of the heat exchanger which has been divided into N cells, each modeled by means of the energy balance equation. It's important to point out that the model considers the storage of thermal energy in the metal parts and the method of discretization, that has been adopted, gives just acceptable results dividing the heat exchanger in a small number of cells. The paper shows some results of the steady-state simulation of a counterflow heat exchanger, as a function of the number of cells, and the effects of some typical transient operating conditions are described.

Keywords— Counterflow, Discretization, Double-pipe Heat Exchanger, Dynamic Simulation, Parallel-flow.

I. INTRODUCTION

NOWADAYS heat exchangers are used in a wide variety of applications and they have to be designed in order to increase their effectiveness without neglecting the costs associated with their life cycle. It's important to predict the heat exchanger behaviour, for both steady-state and transient operating conditions, during the design phase, in order to reduce future possible failures and, consequently, the maintenance costs. The transient simulation is very useful to anticipate some extreme operating conditions which could determine thermal stresses in the metal parts of the heat exchanger.

In this framework the simulation model, described in this paper, represents a flexible Matlab application which can help designer engineers to simulate a double-pipe heat exchanger

under different operating conditions, solving the "rating problem" that is the heat exchanger performance analysis, as in [1]. In fact, knowing the heat exchanger surface geometry and dimensions, fluid flow rates and inlet temperatures, the simulator permits to evaluate the fluid outlet temperatures and the total heat transferred. It is also possible to easily change the inputs, listed above, for the optimal sizing of the heat exchanger which fits a set of desired outlet temperatures.

II. THE DOUBLE-PIPE HEAT EXCHANGER

In the present study a double-pipe heat exchanger has been considered. It consists of two concentric circular tubes: as shown in Fig. 1, one fluid flows inside the inner tube (fluid 1), while the other flows through the annular space (fluid 2).
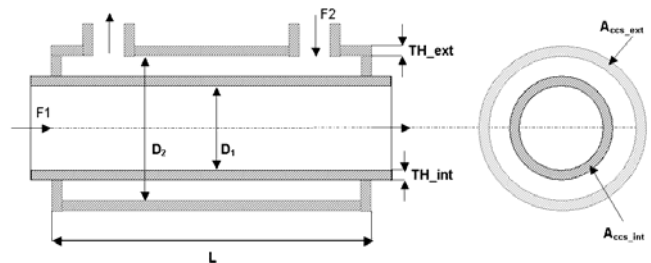
Fig. 1 The double-pipe counterflow heat exchanger

The present analysis considers a double-pipe heat exchanger used to cool, by means of cold water, the lubricating oil, for example in a large industrial gas turbine or a reciprocating internal combustion engine. The water flows inside the inner tube while the oil flows through the annular passage, also called "annulus", as in [1].

A. The discretization of the heat exchanger

In order to simulate the heat exchanger, it has been divided into N cells, as in [2]-[3]. Each of them includes: the cold fluid volume, the metal wall of the inner tube, the hot fluid volume and the metal wall of the outer tube. The geometric dimensions considered in the model are:
- L = length of the heat exchanger
- D_1 = inside diameter of the inner tube
- D_2 = inside diameter of the outer tube
- TH_{int} = thickness of the inner tube

− TH$_{ext}$ = thickness of the outer tube.

The heat exchanger is plugged at the ends by means of a circular cross section drilled plate.

III. THE THERMODYNAMIC MODEL

This section lists the equations used to model the heat exchange between the hot fluid and the cold one inside each of the N cells. The thermodynamic model of the heat exchanger is based on the following assumptions:

− the potential and kinetic energy changes of the two fluids are neglected
− the pressure drops inside the tubes are not taken into consideration
− the heat exchanger is insulated from its surroundings
− the fluids do not undergo a phase change
− the heat exchanger walls are made of a single material, specifically carbon steel
− the temperature of each fluid is uniform over every flow cross section
− the specific heat at constant pressure is constant for each fluid
− the overall heat transfer coefficient is constant throughout the heat exchanger
− inlet temperatures and mass flow rates are known.

A. The cold fluid equations

Fig. 2 shows the simplified scheme that has been adopted to model the mass and heat transfer for the cold fluid in the jth cell. The conservation of energy, in transient conditions, for this subsystem can be written as:

$$\dot{m}_{F1}c_{F1}\left(T_{F1\_in\_j}-T_{F1\_out\_j}\right)+\phi_{F1\_w_{int}\_j}=m_{F1}c_{F1}\frac{\partial T_{F1\_j}}{\partial t} \tag{1}$$

considering the heat flux coming from the internal wall as:

$$\phi_{F1\_w_{int}\_j}=h_{F1}\cdot S_{w\_int\_F1}\cdot\left(T_{w\_int\_j}-T_{F1\_j}\right). \tag{2}$$

$S_{w\,int\,F1}$ is the heat exchange area between the fluid 1 and the wall of the inner tube:

$$S_{w\_int\_F1}=\pi\cdot D_1\cdot\frac{L}{N} \tag{3}$$

and m$_{F1}$ is the mass of fluid 1 inside each cell:

$$m_{F1}=\rho_{F1}\cdot V_{F1}=\rho_{F1}\cdot\pi\cdot\left(\frac{D_1}{2}\right)^2\cdot\left(\frac{L}{N}\right). \tag{4}$$

The model considers that the fluid 1 temperature and the wall temperature of the inner tube inside each cell vary with time only and are constant at the (L/N) length, as in [2].

In order to calculate the heat transfer coefficient h$_{F1}$ the following equation has been adopted:

$$h_{F1}=\frac{k_{F1}\cdot Nu_{F1}}{D_1} \tag{5}$$

considering a fully developed turbulent flow characterized by the Nusselt number calculated by the Dittus-Boelter correlation:

$$Nu_{F1}=0.023\cdot Re_{F1}^{0.8}\cdot Pr_{F1}^{0.3} \tag{6}$$

where the Reynolds and Prandtl numbers are respectively:

$$Re_{F1}=\frac{\rho_{F1}\cdot v_{F1}\cdot D_1}{\mu_{F1}} \tag{7}$$

$$Pr_{F1}=\frac{c_{F1}\cdot\mu_{F1}}{k_{F1}}. \tag{8}$$
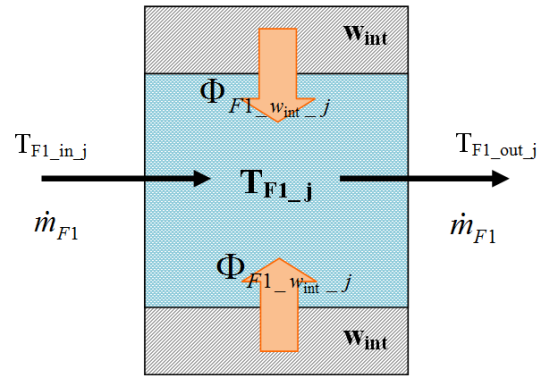
Fig. 2 The mass and heat transfer for the cold fluid

B. The hot fluid equations

Fig. 3 shows the simplified scheme that has been adopted to model the mass and heat transfer for the hot fluid in the jth cell. The conservation of energy, in transient conditions, for this subsystem has been modeled by means of the following differential equation:

$$\dot{m}_{F2}c_{F2}\left(T_{F2\_in\_j}-T_{F2\_out\_j}\right)-\phi_{F2\_w_{int}\_j}-\phi_{F2\_w_{ext}\_j}= \\ =m_{F2}c_{F2}\frac{\partial T_{F2\_j}}{\partial t} \tag{9}$$

where m$_{F2}$ is the mass of fluid 2 inside each cell, $\phi_{F2\_w_{int}\_j}$ is the thermal flux to the internal wall while $\phi_{F2\_w_{ext}\_j}$ is the thermal flux to the external wall:

$$m_{F2}=\rho_{F2}\cdot V_{F2}=\rho_{F2}\cdot\pi\cdot\left(\frac{L}{N}\right)\left[\left(\frac{D_2}{2}\right)^2-\left(\frac{D_1}{2}+TH\_int\right)^2\right] \tag{10}$$

$$\phi_{F2\_w_{int}\_j}=h_{F2}\cdot S_{w\_int\_F2}\cdot\left(T_{F2\_j}-T_{w\_int\_j}\right) \tag{11}$$

$$\phi_{F2\_w_{ext}\_j}=h_{F2}\cdot S_{w\_ext\_F2}\cdot\left(T_{F2\_j}-T_{w\_ext\_j}\right) \tag{12}$$

where:

$$S_{w\_\text{int}\_F2} = \pi \cdot \frac{L}{N} \cdot \left(D_1 + 2 \cdot TH_{\text{int}} \right) \qquad (13)$$

$$S_{w\_ext\_F2} = \pi \cdot D_2 \cdot \frac{L}{N} . \qquad (14)$$

The model assumes that the fluid 2 temperature and the wall temperature of the outer tube inside each cell vary with time only and are constant at the (L/N) length. The heat transfer coefficient h_{F2} has been calculated by means of a procedure similar to that used for fluid 1 but, knowing that in the annulus there is a hydrodinamically developed laminar flow, the following correlation has been adopted in order to evaluate the Nusselt number for the fluid 2, as suggested by [1]:

$$Nu_{F2} = Nu_{\infty} + \left[1 + 0.14 \cdot \left(\frac{D_1 + 2TH_{\text{int}}}{D_2} \right)^{-0.5} \right] \cdot \frac{0.19 \cdot \left(PeD_h / L \right)^{0.8}}{1 + 0.117 \cdot \left(PeD_h / L \right)^{0.467}} \qquad (15)$$

where:

$$Nu_{\infty} = 3.66 + 1.2 \cdot \left(\frac{D_1 + 2TH_{\text{int}}}{D_2} \right)^{-0.5} \qquad (16)$$

$$Pe = Re_{F2} \cdot Pr_{F2} \qquad (17)$$

$$D_h = \frac{\left[D_2^2 - \left(D_1 + 2TH_{\text{int}} \right)^2 \right]}{\left(D_2 + D_1 + 2TH_{\text{int}} \right)} . \qquad (18)$$
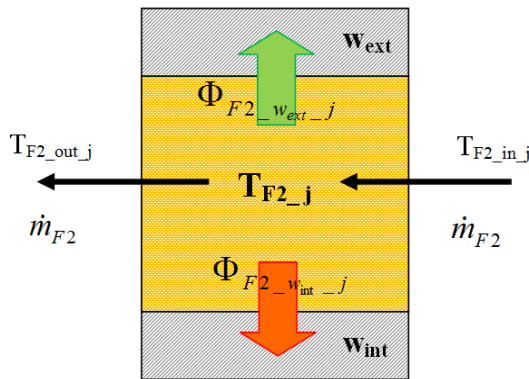
Fig. 3 The mass and heat transfer for the hot fluid

C. The internal and external wall equations

The thermodynamic model considers, for each cell, the storage of thermal energy in the metal parts and so it is possible to evaluate the wall temperature dynamics by the calculation of the thermal fluxes which enter or exit from each portion of the metal wall, as in [4]. Fig. 4 shows a simplified scheme which reports the thermal fluxes for both the internal (inner tube) and external (outer tube) walls.
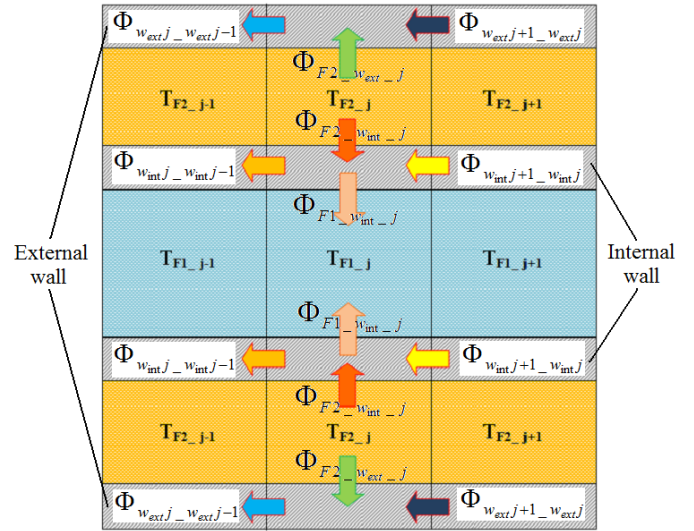
Fig. 4 The thermal fluxes for the internal and external walls

As mentioned above, an uniform wall temperature has been considered for each cell, both for the internal and the external wall. The energy balance equation for the inner tube wall in the jth cell is given by:

$$\phi_{F2\_w_{\text{int}}\_j} - \phi_{F1\_w_{\text{int}}\_j} + \phi_{w_{\text{int}}\_j+1\_w_{\text{int}}\_j} - \phi_{w_{\text{int}}\_j\_w_{\text{int}}\_j-1} =$$
$$= m_{w\_\text{int}} c_w \frac{\partial T_{w\_\text{int}\_j}}{\partial t} \qquad (19)$$

where:

$$\phi_{w_{\text{int}}\_j+1\_w_{\text{int}}\_j} = k_w \cdot \left(\frac{N}{L} \right) \cdot A_{ccs\_int} \cdot \left(T_{w\_int\_j+1} - T_{w\_int\_j} \right) \qquad (20)$$

$$\phi_{w_{\text{int}}\_j\_w_{\text{int}}\_j-1} = k_w \cdot \left(\frac{N}{L} \right) \cdot A_{ccs\_int} \cdot \left(T_{w\_int\_j} - T_{w\_int\_j-1} \right). \qquad (21)$$

$A_{ccs-int}$ is the circular cross section area of the inner tube wall while m_{w-int} is the metal mass of the internal wall within the cell.

On the other hand, the energy balance equation for the outer tube wall in the jth cell is given by:

$$\phi_{F2\_w_{ext}\_j} + \phi_{w_{ext}\_j+1\_w_{ext}\_j} - \phi_{w_{ext}\_j\_w_{ext}\_j-1} =$$
$$= m_{w\_ext} c_w \frac{\partial T_{w\_ext\_j}}{\partial t} \qquad (22)$$

where:

$$\phi_{w_{ext}\_j+1\_w_{ext}\_j} = k_w \cdot \left(\frac{N}{L} \right) \cdot A_{ccs\_ext} \cdot \left(T_{w\_ext\_j+1} - T_{w\_ext\_j} \right) \qquad (23)$$

$$\phi_{w_{ext}\_j\_w_{ext}\_j-1} = k_w \cdot \left(\frac{N}{L}\right) \cdot A_{ccs\_ext} \cdot \left(T_{w\_ext\_j} - T_{w\_ext\_j-1}\right). \tag{24}$$

$A_{ccs\text{-}ext}$ is the circular cross section area of the outer tube wall while $m_{w\text{-}ext}$ is the metal mass of the external wall within the cell.

It's necessary to remember that the external wall is insulated from its surroundings and at the two ends of the heat exchanger, due to the circular cross section drilled plate, the heat exchange between the internal wall and the external wall has been taken into consideration.

D. The heat exchanger effectiveness calculation

The thermodynamic model of the heat exchanger permits also to calculate the log-mean temperature difference ΔT_{lm} and so to evaluate the total heat transfer rate Φ as a function of the overall heat transfer coefficient U and the total heat transfer area:

$$\Phi = U \cdot A \cdot \Delta T_{lm} \tag{25}$$

where the log-mean temperature difference is calculated by means of the two following equations, respectively for the counter-flow (cf) and parallel-flow (pf) heat exchanger, as in [5]:

$$\Delta T_{lm\_cf} = \frac{\left(T_{F2\_in} - T_{F1\_out}\right) - \left(T_{F2\_out} - T_{F1\_in}\right)}{ln\left(\dfrac{T_{F2\_in} - T_{F1\_out}}{T_{F2\_out} - T_{F1\_in}}\right)} \tag{26}$$

$$\Delta T_{lm\_pf} = \frac{\left(T_{F2\_in} - T_{F1\_in}\right) - \left(T_{F2\_out} - T_{F1\_out}\right)}{ln\left(\dfrac{T_{F2\_in} - T_{F1\_in}}{T_{F2\_out} - T_{F1\_out}}\right)}. \tag{27}$$

Knowing the inlet and outlet temperatures of the two fluids, at steady-state operating conditions, the total heat flux has also been calculated as:

$$\Phi = \Phi_{F1} = \Phi_{F2} \tag{28}$$

where:

$$\Phi_{F1} = C_{F1} \cdot (T_{F1\_out} - T_{F1\_in}) = \\ = \dot{m}_{F1}c_{F1}(T_{F1\_out} - T_{F1\_in}) \tag{29}$$

$$\Phi_{F2} = C_{F2} \cdot (T_{F2\_in} - T_{F2\_out}) = \\ = \dot{m}_{F2}c_{F2}(T_{F2\_in} - T_{F2\_out}). \tag{30}$$

The heat exchanger effectiveness (ε) has been calculated as:

$$\varepsilon = \frac{\Phi}{\Phi_{max}} \tag{31}$$

where:

$$\Phi_{max} = C_{min} \cdot (T_{F2\_in} - T_{F1\_in}) . \tag{32}$$

Then the ε-NTU Method has been applied in the simulator, considering the effectiveness as a function of the Number of Transfer Units (NTU) and the ratio (C_{min}/C_{max}) as in [5]-[6]-[7]:

$$\varepsilon = \varepsilon\left(NTU, C_{min}\Big/C_{max}\right) \tag{33}$$

where:

$$NTU = \frac{U \cdot A}{C_{min}}. \tag{34}$$

The correlations used for the calculation of the heat exchanger effectiveness are listed below, as suggested by [5]:

$$\varepsilon_{pf} = \frac{1 - e^{\left[-NTU \cdot \left(1 + \frac{C_{min}}{C_{max}}\right)\right]}}{\left(1 + \dfrac{C_{min}}{C_{max}}\right)} \tag{35}$$

$$\varepsilon_{cf} = \frac{1 - e^{\left[-NTU \cdot \left(1 - \frac{C_{min}}{C_{max}}\right)\right]}}{1 - \left(\dfrac{C_{min}}{C_{max}}\right) \cdot e^{\left[-NTU \cdot \left(1 - \frac{C_{min}}{C_{max}}\right)\right]}}. \tag{36}$$

IV. THE SIMULATION MODEL

The thermodynamic model of the heat exchanger has been implemented in Matlab/Simulink. Two simulators have been created: one for the counterflow heat exchanger and the other for the parallel-flow one. Then, in both simulators, the heat exchanger has been divided in N cells and the discretization process stopped when simulation results seemed to be quite insensitive to the increase of the cells number.

For example, Fig. 5 shows the main window of the simulator for the heat exchanger divided into 5 cells.

Analyzing the above scheme it follows that the main inputs of the simulation model are:
−   the cold fluid mass flow rate
−   the hot fluid mass flow rate
−   the cold fluid inlet temperature
−   the hot fluid inlet temperature.

Then the simulator needs a file input which contains other data such as the heat exchanger geometrical dimensions, the fluids properties (density, thermal conductivity, viscosity,

specific heat), the metal properties (density, thermal conductivity, specific heat) and the initial conditions for the integrator blocks that are the fluids and walls temperatures inside each cell at the simulation start time.

On the other hand, the outputs of the simulator are:
− the exit temperature of the cold fluid
− the exit temperature of the hot fluid
− the cold fluid temperature inside each cell
− the hot fluid temperature inside each cell
− the internal and external wall temperatures inside each cell
− the heat flux exchanged between the two fluids
− the speed of the two fluids.

It is possible to plot all these outputs as a function of time and then the simulator evaluates the heat exchange coefficients by means of the correlations mentioned in Section III.
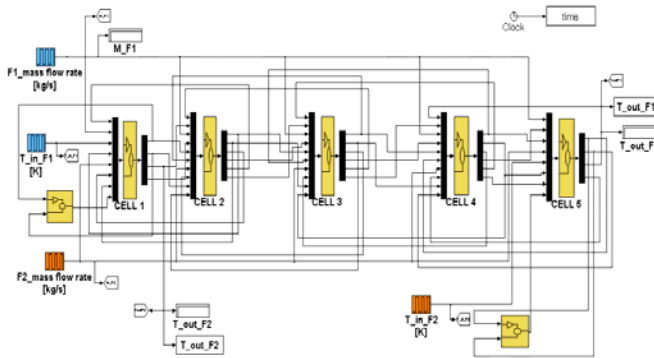
Fig. 5 The main window of the simulator

A. The simulation model of the elementary cell

Fig. 6 shows the simplified scheme of the Simulink subsystem that has been created in order to simulate the jth cell of the heat exchanger.
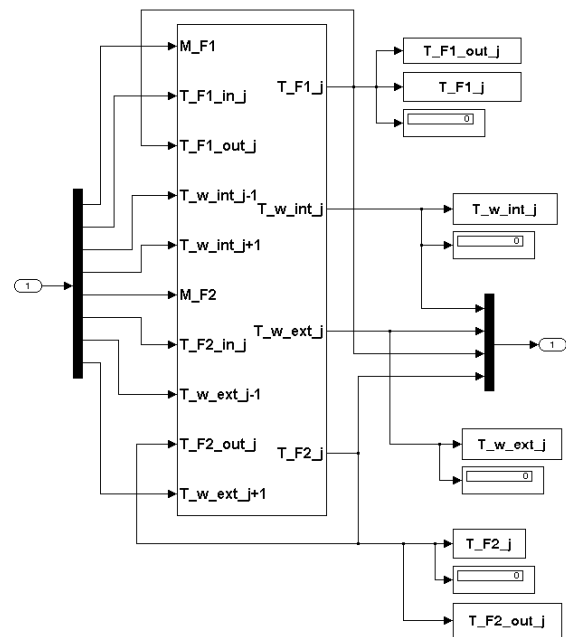
Fig. 6 The elementary cell in the simulation model

The inputs of the jth cell subsystem are:
− the fluid 1 mass flow rate
− the fluid 2 mass flow rate
− the temperatures of the fluids at the cell inlet
− the internal and external wall temperatures in the $(j-1)^{th}$ cell
− the internal and external wall temperatures in the $(j+1)^{th}$ cell
− the temperatures of the fluids at the cell outlet.

The outputs of the jth cell subsystem are:
− the internal and external wall temperatures inside the jth cell
− the fluid 1 and fluid 2 temperatures inside the jth cell
− the temperatures of the fluids at the cell outlet.

The state variables of the jth cell subsystem are:
− the internal and external wall temperatures inside the jth cell
− the fluid 1 and fluid 2 temperatures inside the jth cell.

The fluid 1 and 2 temperatures at the jth cell outlet are assumed to be equal to the fluids temperatures inside the jth cell, that is the state variables.

V. THE SIMULATION RESULTS

This paragraph reports some examples related to several simulations that have been done considering the heat exchanger divided into a variable number of cells; in particular the results refer to four different discretization processes: 5, 10, 15 and 20 cells. The heat exchanger that has been taken as a reference is characterized, as in [8]-[9], by:
− L = 10 m → it is an "equivalent" length because in real operating conditions the heat exchanger is shorter and composed of more than two tubes
− $D_1 = 0.015$ m; $D_2 = 0.03$ m

- $\dot{m}_{F1} = 0.1$ kg/s; $\dot{m}_{F2} = 0.05$ kg/s
- $TF_{1\,in} = 30$ °C; $TF_{2\,in} = 110$ °C.

A. The steady state simulation

In the steady-state simulation phase the model permits to calculate and plot the fluids and walls temperatures for each cell and determine the outlet temperatures of the two fluids, considering the mass flow rates and the inlet temperatures to be constant. The goal of the study has been that of analyzing the variations of the main outputs as a function of the cells number, without changing the heat exchanger's length and diameters.

In this regard Fig. 7, 8, 9, and 10 show the temperatures of the two fluids (hot oil and cold water) and the two walls (internal and external wall) inside each of the N cells which the heat exchanger has been divided in. Each figure indicates also the heat exchanger effectiveness and the temperature differences:

$$\Delta T_{hot} = T_{F2\_in} - T_{F2\_out} \qquad (37)$$

$$\Delta T_{cold} = T_{F1\_out} - T_{F1\_in}. \qquad (38)$$

From the analysis of these graphs it derives that the temperatures calculated by the 5-cells model don't differ much from the ones evaluated by the models characterized by a higher number of cells. Consequently the thermodynamic-simulation model, described in this paper, permits to study accurately the performance of a double-pipe heat exchanger without discretizing it in a large number of cells: so it is possible to save computational time and the simulator is highly flexible and lean.
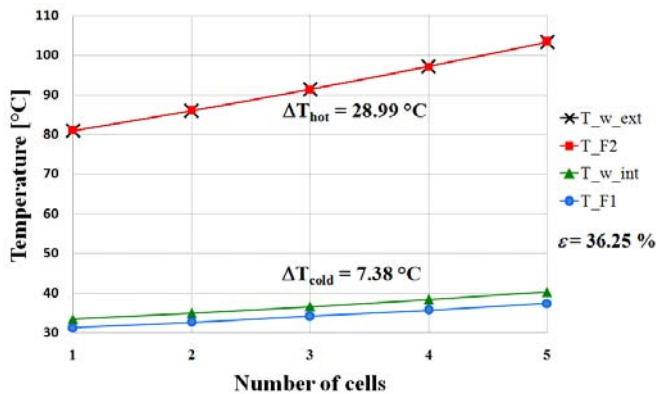
Fig. 7 The temperatures variation for the counterflow heat exchanger divided into 5 cells
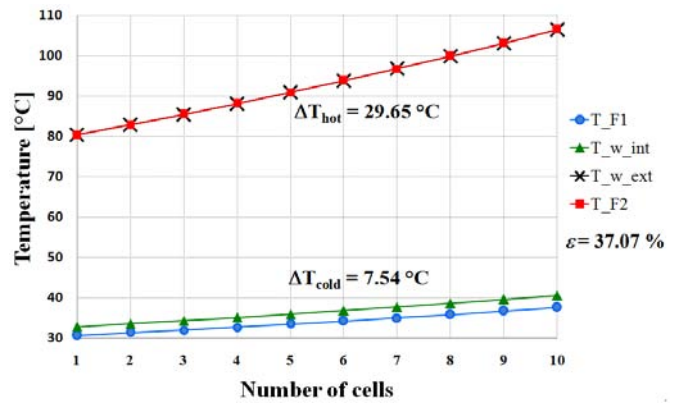
Fig. 8 The temperatures variation for the counterflow heat exchanger divided into 10 cells
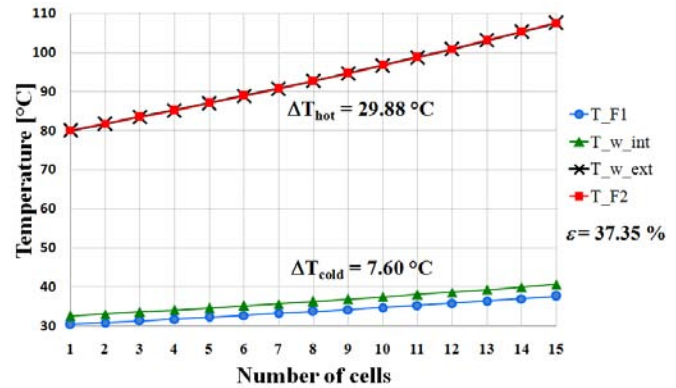
Fig. 9 The temperatures variation for the counterflow heat exchanger divided into 15 cells
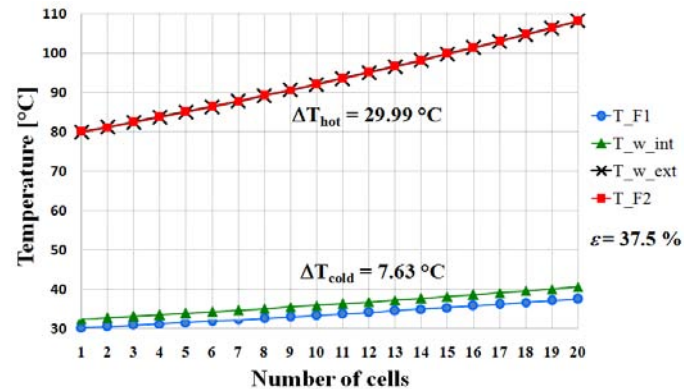
Fig. 10 The temperatures variation for the counterflow heat exchanger divided into 20 cells

Analogous considerations come into play by the analysis of Fig. 11 and 12 which show, more in detail, the temperatures variation of the two fluids as a function of the tube's length considering different number of cells. It is possible to notice that the fluid temperatures vary less and less at the increase in the number of cells.

Similar simulations have been done regarding the parallel-flow heat exchanger and even in that case the output results have shown that the model didn't need a large number of cells in order to predict, with accuracy, the heat exchanger

performance under different operating conditions. For instance, Fig. 13 shows the temperatures variation for the parallel-flow heat exchanger divided into 15 cells. In comparison with the counterflow arrangement, the effectiveness is lower as well as the hot and cold fluids temperature variations along the heat exchanger.

Fig. 13 The temperatures variation for the parallel-flow heat exchanger divided into 15 cells
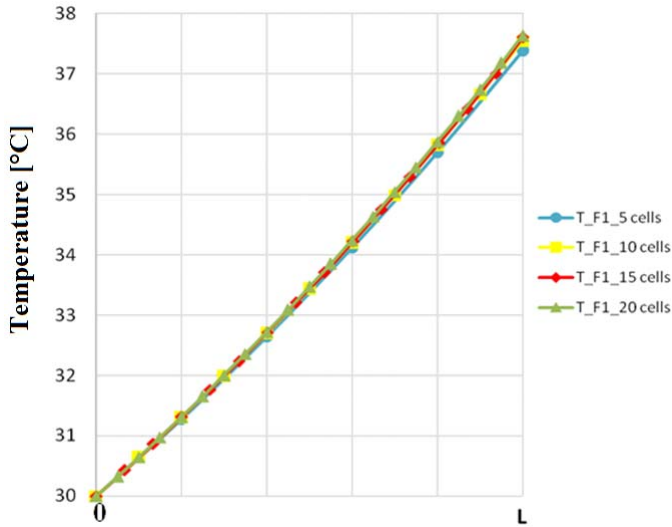
Fig. 11 The cold fluid temperatures variation along the counterflow heat exchanger

As previously mentioned, the results shown in this paragraph refer to an unfinned-tube heat exchanger characterized by an equivalent length of 10 m. Several steady-state simulations have been done varying the heat exchanger's length: as shown in Fig. 14, the decrease of the length determines a higher hot fluid outlet temperature, considering constant (110 °C) the hot fluid inlet temperature.
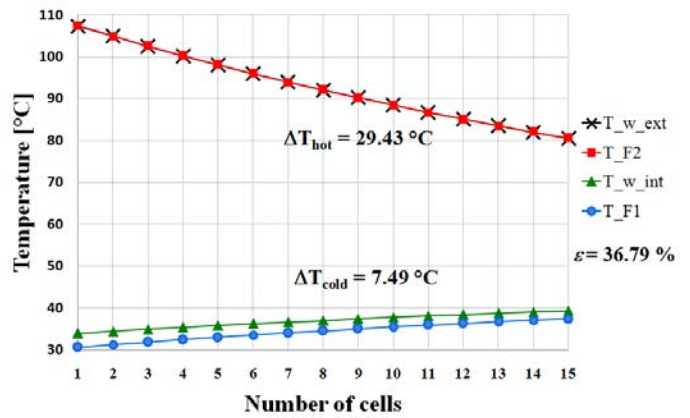
It derives that it is necessary to adopt a finned-tube heat exchanger in order to have a hot fluid outlet temperature equal to 81 °C by means of a double-pipe heat exchanger shorter than 10 m. It is possible to fin both the internal and the external surface of the inner tube; on the other hand the internal and external walls of the outer tube have not to be finned because the heat exchanger is thermally insulated from its surroundings.

So, several simulations have been done varying the size of the surfaces mentioned above: it has been noticed that the adoption of a finned surface for the internal wall of the inner tube does not determine a significant variation of the hot fluid outlet temperature, in comparison with the unfinned solution, while it is very useful to have a finned surface for the external wall of the inner tube.
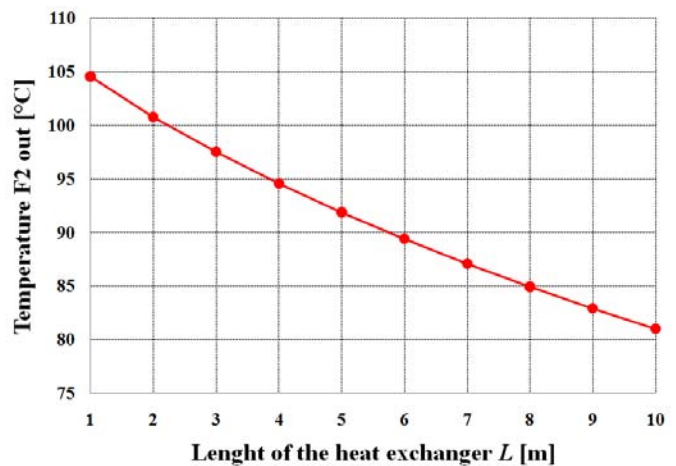
Fig. 14 The hot fluid outlet temperature as a function of the heat exchanger's length

Fig. 12 The hot fluid temperatures variation along the counterflow heat exchanger
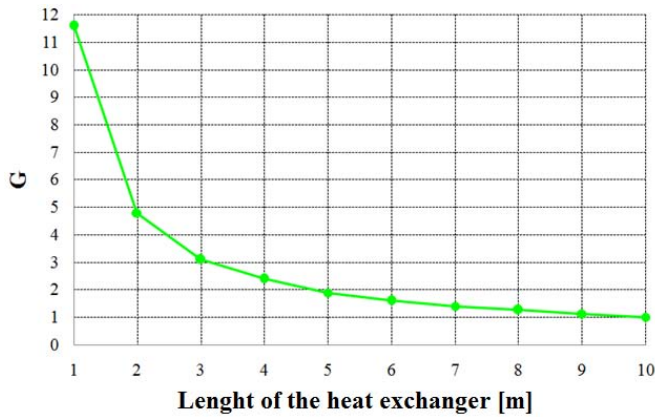
Fig. 15 The ratio between the finned surface and the unfinned one

Knowing that $S_{w\_\text{int}\_F2}$ is the surface of the inner tube external wall, for the unfinned heat exchanger, this surface for the finned heat exchanger can be calculated by:

$$S_{w\_\text{int}\_F2\,finned} = G \cdot S_{w\_\text{int}\_F2} \qquad (39)$$

where G is a multiplying factor. Fig. 15 shows, as a function of the heat exchanger's length, the G values that permit to have a hot fluid outlet temperature equal to 81 °C: if the length L decreases, it is necessary to increase the G factor and so the number of fins.

B. The transient simulation

The simulator can also predict the heat exchanger behaviour, in terms of outlet temperatures of the two fluids and heat fluxes exchanged, for transient operating conditions. For example, it is useful to determine the response of the system to inputs changes such as the increase/decrease of the inlet temperatures or the fluid mass flow rates. It is also possible to evaluate the heat exchanger performance changes considering different wall materials or geometric dimensions. In this Sub-section the simulation of the oil inlet temperature variation is reported, as in [2].

A transient consisting of a step variation of the hot fluid inlet temperature, from 110 °C to 100 °C, has been considered. Consequently, the decrease of the hot fluid outlet temperature has been noticed, from 81 °C to 74.6 °C, as shown in Fig. 16. As a consequence of this temperature variation, there is a remarkable variation of all the other temperatures in the heat exchanger: the graphs in Fig. 17, 18, and 19 outline the internal and external wall temperatures variation as a function of time as well as the decrease in the cold fluid outlet temperature.
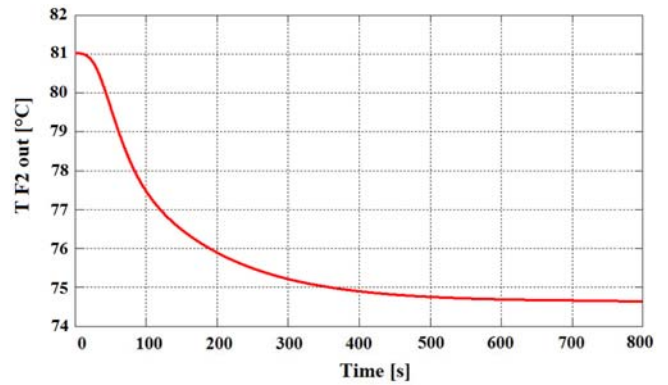
Fig. 16 The hot fluid outlet temperature variation due to the decrease of the hot fluid inlet temperature
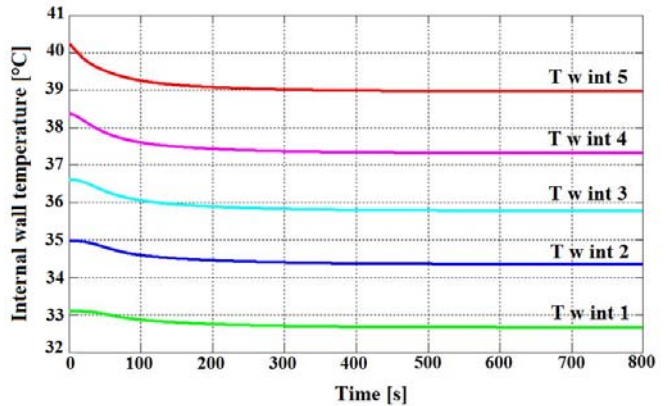
Fig. 17 The internal wall temperatures variation due to the decrease of the hot fluid inlet temperature

In some real operating conditions it is necessary to keep almost constant the hot fluid outlet temperature in spite of extreme flow variations upstream. For the transient above analyzed a PID controller has been implemented in order to maintain costant the hot fluid outlet temperature at about 81 °C by varying the cold fluid mass flow rate, as shown in Fig. 20.

The PID controller automatically finds the correct cold fluid mass flow rate, as reported in Fig. 21 that keeps the hot fluid outlet temperature steady at the set-point.
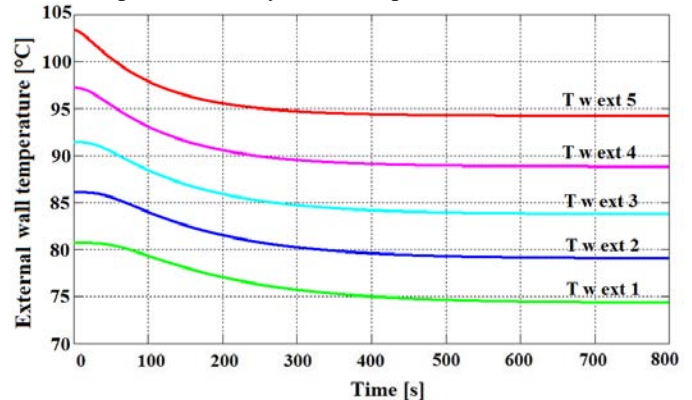
Fig. 18 The external wall temperatures variation due to the decrease

of the hot fluid inlet temperature
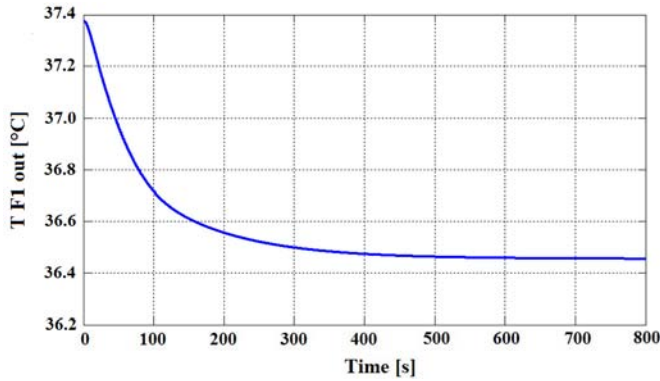
Fig. 19 The cold fluid outlet temperature variation due the decrease of the hot fluid inlet temperature
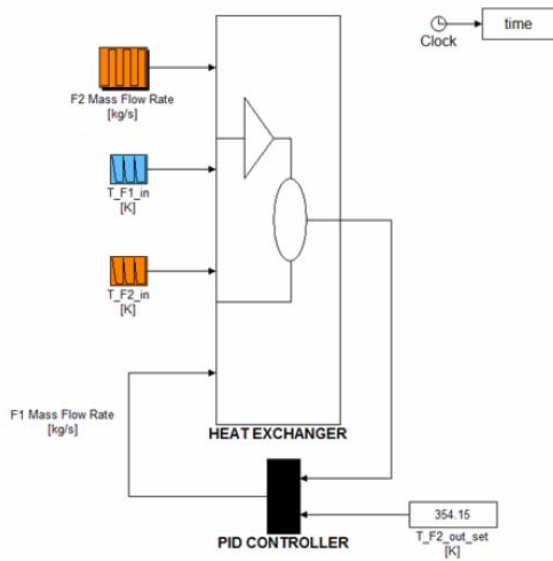
Fig. 20 The PID controller in the Simulink model

The hot fluid outlet temperature initially decreases, according to the lower inlet temperature, then increases because of the cold fluid mass flow rate variation determined by the PID controller. Fig. 22 plots this temperature variation while Fig. 23 shows the increase in the cold fluid exit temperature. It is possible to best fit the time necessary for the hot fluid outlet temperature to be again 81° C by optimizing the PID controller Simulink block parameters which are the proportional, the integral and the derivative terms.
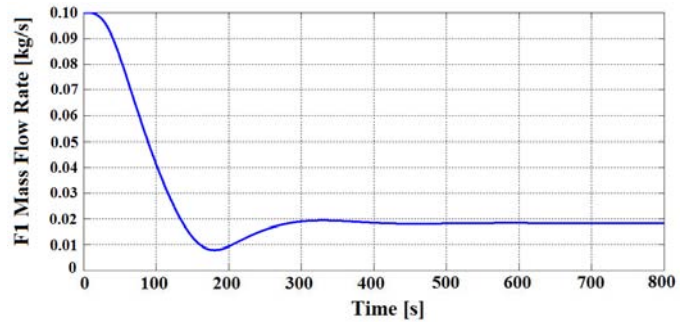
Fig. 21 The cold fluid mass flow rate variation which permits to keep constant the hot fluid outlet temperature
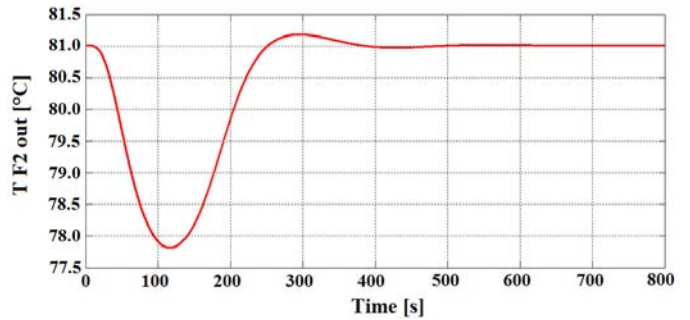
Fig. 22 The hot fluid exit temperature as a function of time
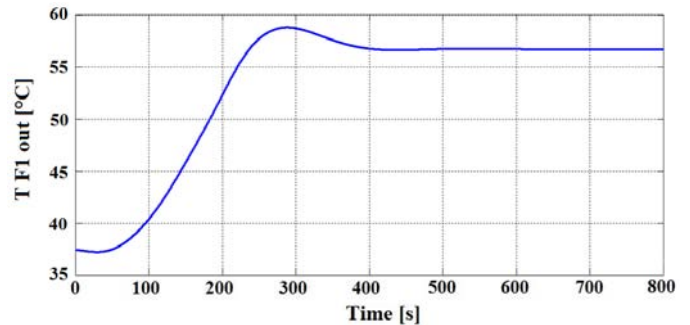
Fig. 23 The cold fluid exit temperature as a function of time

Another important aspect of the study has been that of investigating the effects due to the propagation, throughout the heat exchanger, of a perturbation in temperature, as reported in [10]-[11]-[12]. This analysis has been done considering a double-pipe heat exchanger characterized by the geometrical dimensions and mass flow rates mentioned at the beginning of this paragraph. In particular the analysis has been focused on the effects of the hot fluid inlet temperature variation shown by the first graph reported in Fig. 24: 100 seconds after the simulation start time, the hot fluid inlet temperature decreases from 110 °C to 60 °C, it remains constant for 15 seconds and then increases again to the initial value.
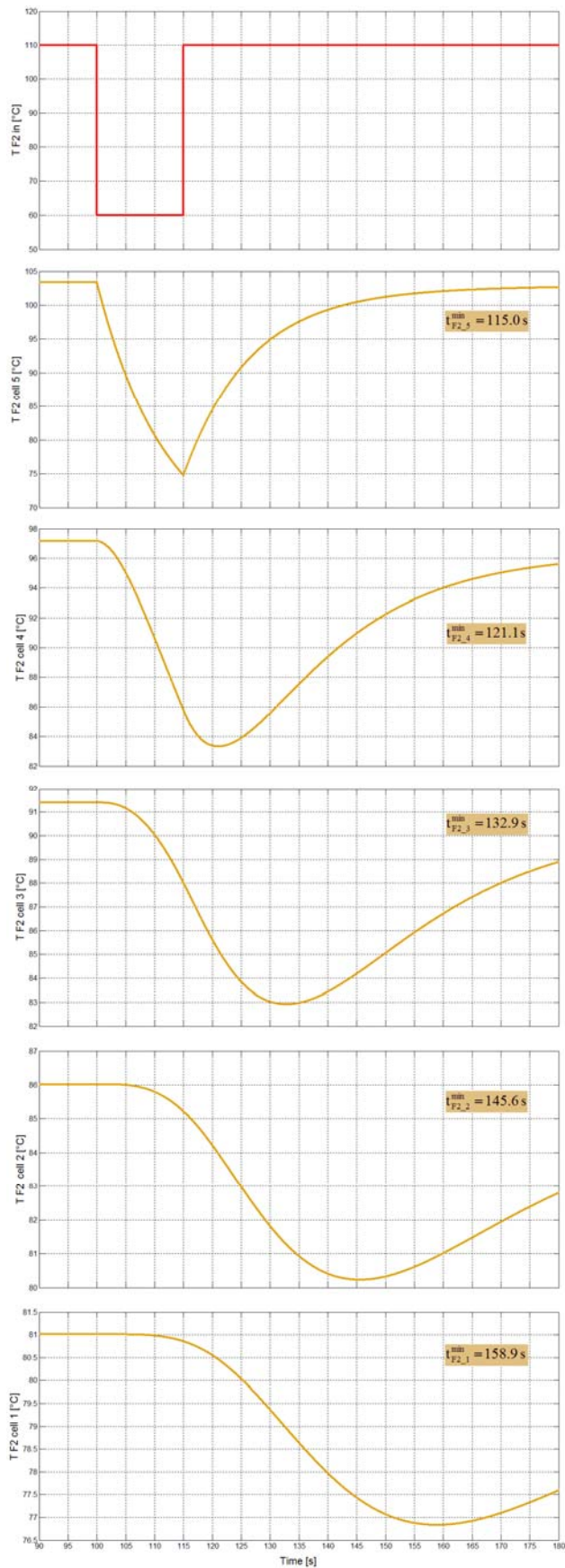
Fig. 24 The propagation of the temperature perturbation through the hot fluid
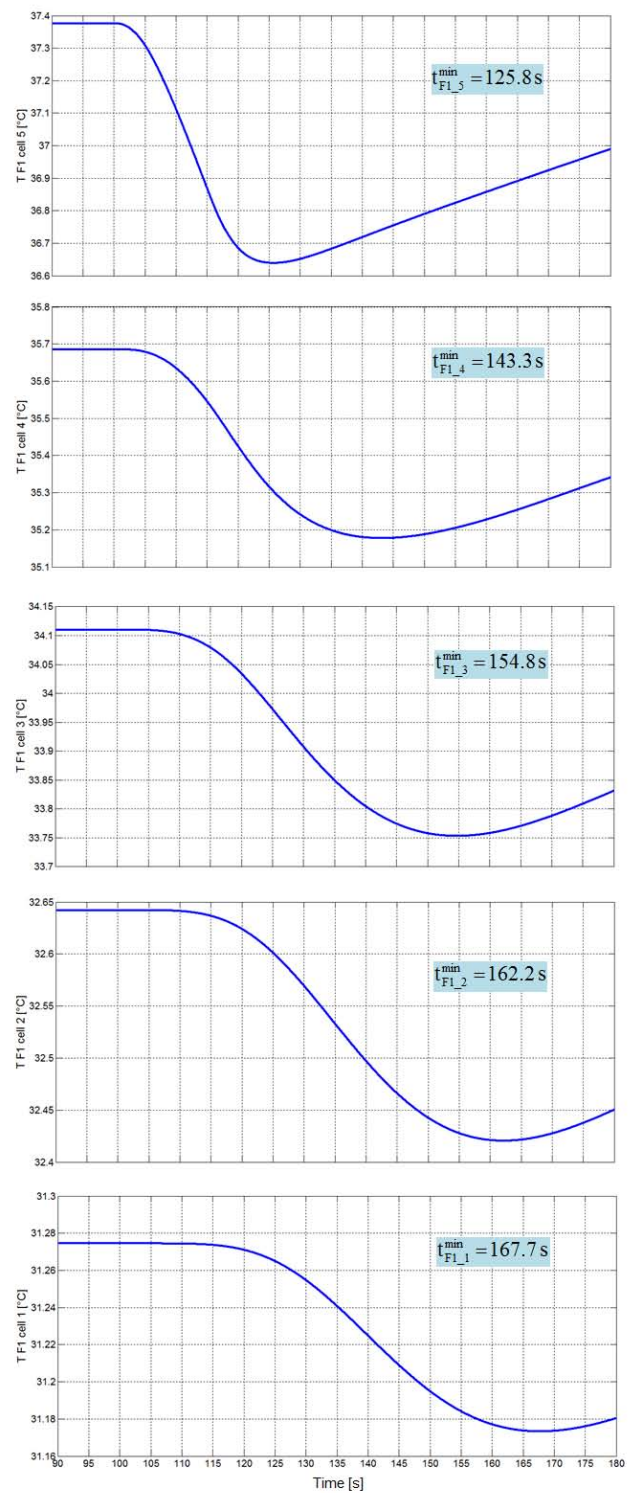
Fig. 25 The propagation of the temperature perturbation through the cold fluid

As a consequence, this perturbation in temperature moves downstream both in the hot and the cold fluid and each cell, which the heat exchanger has been divided in, receives this temperature variation some seconds later the propagation start time. The speed of this perturbation, through the two fluids, depends on the fluids mass flow rates and the heat exchange

physical parameters such as the heat transfer coefficient, the walls thermal conductivity and the walls specific heat. Then the effects of the perturbation differ considering the heat exchanger in counterflow or parallel-flow arrangement.

Fig. 24 shows the hot fluid temperature, inside each cell, as a function of time for the counterflow heat exchanger divided into 5 cells. It's important to calculate the time (t_{F2}^{min}) when the hot fluid temperature reaches the minimum inside each cell: these time values can be related with the speed of the perturbation through the fluid which they refer to. In the example here reported, the perturbation takes about 58.9 seconds to propagate through the hot fluid.

Fig. 25 shows the propagation of the temperature perturbation through the cold fluid: the 5th cell is the first which receives the perturbation because it is close to the inlet of the hot fluid. So, the cold fluid outlet temperature maximum variation occurs 25.8 seconds after the perturbation start time while the temperature of the cold fluid inside the cell 1, which is the cell opposite to the inlet of the hot fluid, assumes the minimum 67.7 later. It derives that the perturbation takes more time to move through the cold fluid than the hot one, because of the thermal storage inside the wall of the inner tube: by this way, the wall temperature dynamics can be considered as a delay time source.

A similar analysis has been done for the parallel-flow heat exchanger: the hot and the cold fluid inlets are closed to the cell 1. Table I reports the time values when both the cold and hot fluid temperatures assume the minimum inside each cell.

TABLE I
THE t^{min} VALUES FOR THE PARALLEL-FLOW HEAT EXCHANGER

Cell number	t_{F1}^{min} [s]	t_{F2}^{min} [s]
Cell 1	120.1	115.0
Cell 2	126.6	121.1
Cell 3	133.7	132.9
Cell 4	140.8	145.6
Cell 5	147.9	158.9

In this case, the cold fluid outlet temperature maximum variation occurs 47.9 seconds after the perturbation start time. It derives that the counterflow heat exchanger has a faster response to inputs variations.

VI. CONCLUSION

The Simulink model, described in this paper, permits to study the heat exchange between two fluids which flow in a double-pipe heat exchanger, that has been divided in N cells in order to be simulated. It is also possible to investigate the response of the heat exchanger to the inputs variation and to determine the effects, in terms of time delays, due to a perturbation in temperature; with regard to the transient simulation, a PID controller has been introduced in the model in order to regulate the hot fluid outlet temperature by means of the cold fluid mass flow rate.

The simulation results, in steady-state and transient conditions, show that the model behaves like a real system just considering a limited number of cells. But it's important to say that a limited number of cells couldn't be sufficient to simulate other types of heat exchangers characterized by another geometry or fluids different from water and oil. As a consequence, the next phase of the present study will be the implementation, inside the simulator, of a flexible algorithm, based on the matricial calculus, in order to automatically divide the heat exchanger into the desired number of cells without manipulating the Simulink blocks structure.

APPENDIX

NOMENCLATURE

Symbol	Quantity	Units
A	Heat exchanger area	m^2
c	Specific heat	J/kgK
C	Specific heat capacity	W/K
D	Diameter	m
h	Heat transfer coefficient	W/m^{2}K
k	Thermal conductivity	W/mK
m	Mass	kg
$\dot{m}$	Mass flow rate	kg/s
L	Lenght	m
N	Number of cells	
NTU	Number of Transfer Units	
Nu	Nusselt number	
Pe	Peclet number	
Pr	Prandtl number	
Re	Reynolds number	
S	Surface	m^2
t	Time	s
T	Temperature	K
TH	Thickness	m
U	Overall heat transfer coefficient	W/m^{2}K
v	Fluid speed	m/s
V	Volume	m^3

Greek Symbol	Quantity	Units
ε	Effectiveness	
φ	Thermal flux	W
μ	Viscosity	Pa·s
ρ	Density	kg/m^3

Subscript	Description
ccs	circular cross section
cf	counterflow
ext	external
F1	Fluid 1
F2	Fluid 2
h	hydraulic
in	inlet
int	internal
j	index for the jth cell
lm	log-mean
max	maximum
min	minimum
pf	parallel-flow
out	outlet
w	wall

REFERENCES

[1] S. Kakac, H. Liu, *Heat Exchangers: Selection, Rating and Thermal Design*, Second Edition, CRC Press, 2002.

[2] M.R. Ansari, V. Mortazavi, "Simulation of dynamical response of a countercurrent heat exchanger to inlet temperature or mass flow rate change," *Applied Thermal Engineering*, 26 (2006), pp. 2401-2408.

[3] A. Zavala-Rìo, R. Santiesteban-Cos, "Reliable compartmental models for double-pipe heat exchangers: an analytical study," *Applied Mathematical Modelling*, 31 (2007), pp. 1739-1752.

[4] A. W. Ordys, A. W. Pike, M. A. Johnson, R. M. Katebi, M. J. Grimble, *Modelling and Simulation of Power Generation Plants*, Springer-Verlag, London, 1994.

[5] G. Guglielmini, C. Pisoni, *Elementi di Trasmissione del Calore*, Editoriale Veschi, Milano, 1990.

[6] G. Comino, G. Cortella, G. Croce, *Energetica Generale*, IV Edizione, Servizi Grafici Editoriali snc, Padova, 2005.

[7] C. Bonacina, A. Cavallini, L. Mattarolo, *Trasmissione del Calore*, Cleup Editore, Padova, 1992.

[8] G. Cornetti, *Macchine a Fluido*, Edizioni Il Capitello, Torino, 1997.

[9] G. Guglielmini, E. Nannei, C. Pisoni, *Problemi di Termodinamica Tecnica e di Trasmissione del Calore*, Ecig, Genova, 1993.

[10] W. F. Stoecker, *Design of Thermal Systems*, McGraw-Hill International Editions, 1989.

[11] J. Yin, M. K. Jensen, "Analytic model for transient heat exchanger response," *International Journal of Heat and Mass Transfer*, 46 (2003), pp. 3255-3264.

[12] M. Mishra, P. K. Das, S. Sarangi, "Transient behaviour of crossflow heat exchangers due to perturbations in temperature and flow," *International Journal of Heat and Mass Transfer*, 49 (2006), pp. 1083-1089.